

**PREPARATION AND CHARACTERIZATION OF
ELECTROSPUN CERAMIC NANOFIBERS INTO
POLYIMIDE COMPOSITE FILMS**

MENG SOPHEAK

UNIVERSITI SAINS MALAYSIA

2017

**PREPARATION AND CHARACTERIZATION OF ELECTROSPUN
CERAMIC NANOFIBERS INTO POLYIMIDE COMPOSITE FILMS**

by

MENG SOPHEAK

**Thesis submitted in fulfillment of
the requirements for the degree of
Master of Science**

July 2017

ACKNOWLEDGEMENTS

First and foremost, I would like to express my sincere appreciation to my supervisor, Prof. Dr. Zulkifli bin Ahmad, for his valuable guidance, motivation and advice while working in this project. He always believed in my ability and kept pushing my limit in order to bring out my best self. I also would like to extend my gratitude to my co-supervisors, Prof. Dr. Hanafi Ismail and Dr. Tan Soon Huat, who has given me a very helpful advice and valuable comments.

I would like to acknowledge to my scholarship sponsor AUN/SEED-Net for its financial support (Grant no – 6050315) during my master program. I also would like to express my gratitude to Dean, Deputy Dean, lecturers, technicians and all staffs of School of Materials and Mineral Resources Engineering (SMMRE) for their kind assistants and supports. Many thanks to Universiti Sains Malaysia (USM) and SMMRE for research facilities.

Finally, I must express my very profound gratitude to my beloved parents and my family for encouraging and supporting me throughout my years of study and through the process of researching and writing this thesis. Special thanks to all my friends, especially Mr. Lim Kar Wai, who helped me greatly during my study years at Universiti Sains Malaysia (USM).

TABLE OF CONTENTS

	Page
ACKNOWLEDGEMENTS	ii
TABLE OF CONTENTS	iii
LIST OF TABLES	vii
LIST OF FIGURES	viii
LIST OF ABBREVIATIONS	xiv
LIST OF SYMBOLS	xvi
ABSTRAK	xviii
ABSTRACT	xix
CHAPTER ONE: INTRODUCTION	
1.1 Research background	1
1.2 Problem statements	3
1.3 Objectives of the study	4
1.4 Scope of the study	4
CHAPTER TWO: LITERATURE REVIEW	
2.1 Dielectric material	6
2.2 Dielectric polarization	7
2.3. Dielectric constant	10
2.4 Dielectric loss	11
2.5 Dielectric application	13
2.6 Polyimide	13
2.6.1 One-step method synthesis	14
2.6.2 Two-steps method synthesis	15
2.7 Ceramic fillers	17
2.7.1 Barium titanate	17
2.7.2 Titanium oxide	18
2.7.3 Zirconium oxide	19
2.8 Polyimide/ ceramic composites	21
2.8.1 PI/BaTiO ₃	21
2.8.2 PI/TiO ₂	22
2.8.3 PI/ZrO ₂	23
2.9 Electrospinning	23
2.9.1 Set up and operation principle	23
2.9.2 Effects of various parameters on electrospinning	25

2.9.3	Electrospun ceramic nanofibers	27
-------	--------------------------------	----

CHAPTER THREE: METHODOLOGY

3.1	Raw Material	29
3.1.1	2,2-Bis[4-(4-aminophenoxy)phenyl]propane (BAPP)	29
3.1.2	3,3',4,4'-Biphenyltetracarboxylic dianhydride (BPDA)	29
3.1.3	N-Methyl-2-pyrrolidone (NMP)	29
3.1.4	Barium carbonate	29
3.1.5	Titanium (IV) isopropoxide	29
3.1.6	Zirconium(IV) acetylacetonate	30
3.1.7	Polyvinylpyrrolidone (PVP)	30
3.2	Ceramic nanofibers preparation	30
3.2.1	BaTiO ₃ nanofibers (BT-NF)	31
3.2.2	TiO ₂ nanofibers (Ti-NF)	31
3.2.3	ZrO ₂ nanofibers (Zr-NF)	32
3.3	Purification of NMP	32
3.4	Synthesis of poly (amic acid) (PAA)	33
3.5	Preparation of PI film	33
3.6	Preparation of PI/ceramic fibers composite by <i>In-situ</i> polymerization	34
3.7	Characterization	35
3.7.1	Fourier transform infrared (FTIR) Analysis	35
3.7.2	X-ray diffraction (XRD)	35
3.7.3	Scanning electron microscopy (SEM)	36
3.7.4	Thermogravimetric analysis (TGA)	36
3.7.5	Differential scanning calorimetry (DSC)	36
3.7.6	Dielectric measurement	36

CHAPTER FOUR: RESULTS AND DISCUSSION

4.1	Characterization of ceramic nanofibers	38
4.1.1	Microstructure	38
4.1.1(a)	BaTiO ₃ nanofibers (BT-NF)	38
4.1.1(b)	TiO ₂ nanofibers (Ti-NF)	40
4.1.1(c)	ZrO ₂ nanofibers (Zr-NF)	42
4.1.2	Fourier transform infrared (FTIR)	43
4.1.2(a)	BT-NF	43
4.1.2(b)	Ti-NF	44
4.1.2(c)	Zr-NF	45

4.1.3	X-ray diffraction (XRD)	46
4.1.3(a)	BT-NF	46
4.1.3(b)	Ti-NF	47
4.1.3(c)	Zr-NF	48
4.2	Effect of <i>in-situ</i> polymerization on distribution of nanofiber in the composite	49
4.3	Characterization of composite films	50
4.3.1	Microstructure analysis (SEM)	50
4.3.1(a)	PI/BT-NF	50
4.3.1(b)	PI/Ti-NF	51
4.3.1(c)	PI/Zr-NF	53
4.3.2	FTIR analysis	54
4.3.2(a)	Poly (amic acid) and polyimide	54
4.3.2(b)	PI/BT-NF	55
4.3.2(c)	PI/Ti-NF	56
4.3.2(d)	PI/Zr-NF	57
4.3.3	Crystal structure (XRD)	57
4.3.3(a)	PI/BT-NF	57
4.3.3(b)	PI/Ti-NF	59
4.3.3(c)	PI/Zr-NF	60
4.3.4	Dielectric properties	62
4.3.4(a)	PI/BT-NF	62
4.3.4(b)	PI/Ti-NF	64
4.3.4(c)	PI/Zr-NF	66
4.3.4(d)	PI/ceramic nanofiber composite	68
4.3.5	Thermal analysis	69
4.3.5(a)	PI/BT-NF	69
4.3.5(b)	PI/Ti-NF	72
4.3.5(c)	PI/Zr-NF	74
4.3.5(d)	PI/ceramic nanofiber composites	76
4.3.6	Comparison properties between commercial dielectric material with materials in present study	78

CHAPTER FIVE: CONCLUSION AND SUGGESTIONS

5.1	Conclusion	80
5.2	Suggestions for future work	81

REFERENCES

82

APPENDICES

Appendix A: List of Attended Conferences

LIST OF TABLES

		Page
Table 2.1	Dielectric constant and dielectric loss of selected materials at 1kHz and room temperature	11
Table 2.2	Parameters of electrospinning and their effect on electrospinning process and morphology of fibers	25
Table 4.1	Decomposition temperature, char yield and limiting oxygen index of pure PI and PI/BT-NF composites	72
Table 4.2	Decomposition temperature, char yield and limiting oxygen index of Pure PI and PI/Ti-NF composites	74
Table 4.3	Decomposition temperature, char yield and limiting oxygen index of Pure PI and PI/Zr-NF composites	76
Table 4.4	Comparison properties between commercial dielectric material from 3M Embedded capacitance material with present study	79

LIST OF FIGURES

		Page
Figure 2.1	Frequency dependence of polarization process (Rajendran, 2010)	8
Figure 2.2	Frequency dependence of (a) dielectric constant and (b) dielectric loss (Barsoum, 2003)	12
Figure 2.3	Reaction scheme of poly(amic acid) and polyimide	16
Figure 2.4	A unit cells for the perovskite structure of BaTiO ₃ (Viswanathan, 2006)	18
Figure 2.5	Unit cells (top) and crystal structures (bottom) of (a) rutile, (b) anatase and (c) brookite (Khataee and Mansoori, 2011)	19
Figure 2.6	Crystal phase and unit cell of Zirconium oxide (Glidewell Laboratories, 2016)	20
Figure 2.7	Typical electrospinning set up (Haghi, 2011)	24
Figure 3.1	Diagram of ceramic nanofiber preparation	30
Figure 3.2	The <i>in-situ</i> polymerization of PI/ceramic nanofibers composite	34
Figure 4.1	SEM micrograph of As-spun BT-NF with feed rate of 1 ml/h, tip-to-collector distance of 12 cm and voltage of (a) 12kV and (b) 18 kv	39
Figure 4.2	SEM micrographs and diameter distribution graphs of (a) as-spun BT-NF and (b) BT-NF after calcination at 800 °C	39

Figure 4.3	SEM micrograph of as-spun Ti-NF using an applied voltage of 15 kV and tip-to-collector distance of 20 cm with feed rate of 1.5 ml/h	41
Figure 4.4	SEM micrographs of Ti-NF with 10 kX magnification (a) before and (b) after calcination and 20 kX magnification (c) before and (d) after calcination at 850 °C. Diameter distributions graph of Ti-NF (e) before and (f) after calcination	41
Figure 4.5	SEM micrographs of Zr-NF with 10 KX magnification (a) before and (b) after calcination and 20 KX magnification (c) before and (d) after calcination at 550 °C. Diameter distributions graph of Zr-NF (e) before and (f) after calcination	42
Figure 4.6	FTIR spectra of as-spun and calcined BT-NF	44
Figure 4.7	FTIR spectra of as-spun and calcined Ti-NF	45
Figure 4.8	FTIR spectra of as-spun and calcined Zr-NF	46
Figure 4.9	XRD diffractogram of BT-NF calcined at 800°C	47
Figure 4.10	XRD diffractogram of Ti-NF calcined at 850°C	48
Figure 4.11	XRD diffractogram of Zr-NF calcined at 550°C	49
Figure 4.12	SEM micrograph of PI/Zr-NF (20 wt%) composite film with uniform dispersion prepared by <i>in-situ</i> polymerization and ultrasonication	50

Figure 4.13	SEM micrograph of (a) pure polyimide, PI/BT-NF with nanofiber content of (b) 5 wt%, (c) 10 wt%, (d) 15 wt% and (e) 20 wt% as well as (f) the length distribution graph of BT-NF	51
Figure 4.14	SEM micrograph of (a) pure polyimide, PI/Ti-NF with nanofiber content of (b) 5 wt%, (c) 10 wt%, (d) 15 wt% and (e) 20 wt% as well as (f) the length distribution graph of Ti-NF	52
Figure 4.15	SEM micrograph of (a) pure polyimide, PI/Zr-NF with nanofiber content of (b) 5 wt%, (c) 10 wt%, (d) 15 wt% and (e) 20 wt% as well as (f) the length distribution graph of Zr-NF	53
Figure 4.16	FTIR spectra of PAA and PI	55
Figure 4.17	FTIR spectra of Pure PI, BT-NF and PI/BT-NF with nanofiber content of 5 wt%, 10 wt%, 15 wt% and 20 wt%	55
Figure 4.18	FTIR spectra of Pure PI, Ti-NF and PI/Ti-NF with nanofiber content of 5 wt%, 10 wt%, 15 wt% and 20 wt%	56
Figure 4.19	FTIR spectra of Pure PI, Zr-NF and PI/Zr-NF with nanofiber content of 5 wt%, 10 wt%, 15 wt% and 20 wt%	57
Figure 4.20	XRD patterns of pure PI and PI/BT-NF with nanofiber concentration of 5, 10, 15, 20 and 100wt%.	58
Figure 4.21	XRD patterns of pure PI and PI/Ti-NF with nanofiber concentration of 5 wt%, 10 wt%, 15 wt%, 20 wt% and 100 wt% at 2θ from 29° to 34°	59

Figure 4.22	XRD patterns of pure PI and PI/Ti-NF with nanofiber concentration of 5 wt%, 10 wt%, 15 wt%, 20 wt% and 100 wt%	59
Figure 4.23	XRD patterns of pure PI and PI/Ti-NF with nanofiber concentration of 5 wt%, 10 wt%, 15 wt%, 20 wt% and 100 wt% at 2θ from 21° to 31°	60
Figure 4.24	XRD patterns of pure PI and PI/Zr-NF with nanofiber concentration of 5 wt%, 10 wt%, 15 wt%, 20 wt% and 100 wt%	61
Figure 4.25	XRD patterns of pure PI and PI/Zr-NF with nanofiber concentration of 5 wt%, 10 wt%, 15 wt%, 20 wt% and 100 wt% at 2θ from 42° to 58°	61
Figure 4.26	The effect of BT-NF content on dielectric constant and dielectric loss of PI/BT-NF composite films at frequency range from 100Hz to 1MHz and measured at room temperature	63
Figure 4.27	Frequency dependence of (a) dielectric constant and (b) dielectric loss of PI/BT-NF composite films with concentration of 0 wt%, 5 wt%, 10 wt%, 15 wt% and 20 wt%	64
Figure 4.28	Dielectric constant and dielectric loss of PI/Ti-NF composite films as a function of Ti-NF concentration at frequency range from 100Hz to 1MHz and measured at room temperature (25°)	65
Figure 4.29	Frequency dependence of (a) dielectric constant and (b) dielectric loss of PI/Ti-NF composite films with concentration of 0 wt%, 5 wt%, 10 wt%, 15 wt% and 20wt%	66

Figure 4.30	Dielectric constant and dielectric loss of PI/Zr-NF composite films as a function of Zr-NF concentration at frequency range from 100 Hz to 1 MHz and measured at room temperature	67
Figure 4.31	Dielectric constant and dielectric loss of PI/Zr-NF composite films as a function of Zr-NF concentration at frequency range from 100Hz to 1MHz and measured at room temperature	68
Figure 4.32	(a) The effect of nanofiber concentration on the dielectric constant PI/BT-NF, PI/Ti-NF and PI/Zr-NF composite films at frequency 1MHz and (b) the effect of sweeping frequency on dielectric loss of the composite films at 20wt% concentration	69
Figure 4.33	DSC graph of neat PI and PI/BT-NF with nanofiber concentration of 5 wt%, 10 wt%, 15 wt% and 20 wt%	70
Figure 4.34	TGA graphs of pure PI and PI/BT-NF with nanofiber concentration of 5 wt%, 10 wt%, 15 wt% and 20 wt%	71
Figure 4.35	DSC graphs of PI and PI/Ti-NF with nanofiber concentration of 5 wt%, 10 wt%, 15 wt% and 20 wt%	73
Figure 4.36	TGA graphs of pure PI and PI/Ti-NF with nanofiber concentration of 5 wt%, 10 wt%, 15 wt% and 20 wt%	74
Figure 4.37	DSC graphs of pure PI and PI/Zr-NF with nanofiber concentration of 5 wt%, 10 wt%, 15 wt% and 20 wt%	75
Figure 4.38	TGA graphs of pure PI and PI/Zr-NF with nanofiber concentration of 5 wt%, 10 wt%, 15 wt% and 20 wt%	76

Figure 4.39 TGA graphs of pure PI, PI/BT-NF, PI/Ti-NF and PI/Zr-NF composite film with 20 wt%

77

LIST OF ABBREVIATIONS

Al ₂ O ₃	Aluminium Oxide/Alumina
APTS	3-aminopropyltriethoxysilane
BAPP	2,2-Bis [4-(4-aminophenoxy)phenyl]propane, 4,4'-(4,4'- Isopropylidenediphenyl-1,1'-diyldioxy)dianiline
BaCO ₃	Barium carbonate
BaTiO ₃	Barium titanate
BPDA	3,3',4,4'-Biphenyltetracarboxylic dianhydride
BT-NF	Barium titanate nanofibers
CR	Char Yield
DSC	Different Scanning Calorimetry
FTIR	Fourier Transform Infrared
LCR	Inductance (L), Capacitance (C), Resistance (R)
NMP	N-Methyl-2-pyrrolidone
PAA	Poly(amic acid)
PE	Polyethylene
PI	Polyimide
PP	Polypropylene
PVP	Polyvinylpyrrolidone
PVDF	Poly(vinylidene fluoride)
SEM	Scanning Electron Microscopy
TGA	Thermogravimetric Analysis
TiO ₂	Titanium Oxide/ Titania
Ti-NF	Titanium Oxide nanofibers
TTIP	Titanium (IV) isopropoxide
XRD	X-Ray Diffraction
ZrO ₂	Zirconium Oxide/ Zirconia

Zr-NF

Zirconium Oxide nanofibers

LIST OF SYMBOLS

%	Percent
°	Degree
°C	Degree Celsius
°C/min	Degree Celsius per minute
A	Contact area
C'	Capacitance of a material
C	Capacitance of a vacuum
cm	Centimeter
d	Distance
E	Electric field
f	Farads
g/mol	Gram per mole
h	Hour
Hz	Hertz
K	Dielectric constant
kV	Kilo-Voltage
kHz	Kilo-hertz
MHz	Mega-hertz
min	Minute
ml	Millitre
ml/h	Millitre per hour
mol	Mole
M _w	Average molecular weight
N	Number of particles in unit volume
nm	Nanometer
Q,q	Charge

p	Dipole moment
P	Polarization
T_g	Glass transition temperature
T_5	Decomposition temperature at 5% weight loss
T_{10}	Decomposition temperature at 10% weight loss
Wh/kg	Watt hour per kilogram
wt%	Weight percent
μm	Micro meter
ε	Permittivity of a material
ε_0	Permittivity of a vacuum
α	Polarizability
α_e	Electronic polarizability
α_i	Ionic polarizability
α_d	Dipolar polarizability
α_s	Space charge polarizability

PENYEDIAAN DAN PENCIRIAN GENTIAN-NANO SERAMIK ELEKTROSPIN DALAM FILEM KOMPOSIT POLIIMIDA

ABSTRAK

Kebelakangan ini, banyak penyelidikan tertumpu kepada bahan-bahan satu dimensi seperti gentian-nano untuk meningkatkan sifat-sifat dielektrik komposit disebabkan keunikan sifat. Dalam kajian ini, filem komposit poliimida/gentian-nano seramik telah dihasilkan dengan percampuran pelbagai jenis gentian-nano seramik (BaTiO_3 , TiO_2 dan ZrO_2) dalam matrik poliimida berasaskan 2,2-Bis[4-(4-aminofenoksi)fenil]propana (BAPP) and 3,3',4,4'-Bifenil tetrakarboksilik dianhidrida (BPDA). Gentian-nano seramik telah disediakan oleh gabungan proses sol-gel, pemutaran-elektro dan pengkalsinan sebelum percampuran dengan poliimida melalui pempolimeran *in situ* dibantu oleh ultrasonik. Jelmaan Fourier inframerah (FTIR), Pembelauan Sinar-X (XRD), Mikroskopi imbasan elektron (SEM), Penganalisa impedence (meter LCR), pengimbasan kalorimeter pembeza (DSC) dan analisis gravimetrik terma (TGA) telah digunakan untuk mencirikan sifat-sifat filem komposit seperti struktur kimia, fasa kristal, morfologi, dielektrik dan sifat haba. Spektra FTIR menunjukkan puncak berciri kumpulan imida dalam filem komposit serta puncak penyerapan sepadan dengan gentian-nano seramik. Diffractogram XRD menunjukkan filem komposit mempamerkan struktur kristal sama dengan gentian-nano seramik induk. Keputusan daripada mikrograf SEM menunjukkan gentian-nano seramik juga tersebar dalam filem komposit kerana nisbah aspek besar dan kaedah ultrasonik. Pemalar dielektrik PI/ BaTiO_3 (20 wt%) adalah 6.78 dengan kehilangan dielektrik rendah bernilai 0.009 pada 1 MHz dan suhu bilik. Akhir sekali, semua filem komposit juga menunjukkan kestabilan terma yang tinggi.

PREPARATION AND CHARACTERIZATION OF ELECTROSPUN CERAMIC NANOFIBERS INTO POLYIMIDE COMPOSITE FILMS

ABSTRACT

Recently, many researchers have focused on one-dimensional materials such as nanofibers to enhance dielectric properties of the composites due to the unique properties. In this study, polyimide/ceramic nanofibers composite films were prepared by incorporating various types of ceramic nanofibers (BaTiO_3 , TiO_2 and ZrO_2) to polyimide matrix derived from 2,2-Bis[4-(4-aminophenoxy)phenyl]propane (BAPP) and 3,3',4,4'-Biphenyl tetracarboxylic dianhydride (BPDA). The ceramic nanofibers were prepared by the combination of sol-gel process, electrospinning and calcination before incorporating with polyimide via *in-situ* polymerization assisted by ultrasonication. Fourier transform infrared (FTIR), X-ray diffraction (XRD), Scanning electron microscopy (SEM), impedance analyzer (LCR meter), Differential Scanning calorimetry (DSC) and thermal gravimetric analysis (TGA) were used to characterize properties of composite films such as chemical structure, crystal phase, morphology, dielectric and thermal properties. FTIR spectra showed the characteristic peaks of the imide groups in the composite films as well as absorption bands corresponding to ceramic nanofibers. XRD diffractograms demonstrated the composite films exhibited the crystal structure similar to those of their parent ceramic nanofibers. The results from SEM micrographs indicated ceramic nanofibers were well dispersed in the composite films due to their large aspect ratio and ultrasonication method. Dielectric constant of the PI/ BaTiO_3 (20 wt%) is 6.78 (about 2 times of pure polyimide) with low dielectric loss of 0.009 at 1 MHz and room temperature. Lastly, all of the composite films also showed high thermal stability.

CHAPTER ONE

INTRODUCTION

1.1 Research background

Electronic industry is one of the industry sectors, which experience rapid growth over the last century and becomes a global industry worth billions of dollars. With the development of electronic technology, miniaturization, higher efficiency and lower production cost are greatly preferable for electronic components and products. Electronic products are getting smaller and lighter in order to keep up with the demand of the consumers. In addition, those products are designed to be multifunctional and good performance even in extreme condition such as higher temperature. Most of the electronic products like electronic circuit usually consists of basic electronic components such as capacitor, inductor, resistor and transistor.

Dielectric materials are commonly used in fabricating electronic components such as capacitor and dielectric resonator. Since miniaturization is favourable for advancement of electronic technology, some dielectric materials are produced in thin film shape due to its flexibility and smaller size. Currently, polymer-based dielectrics are widely used in electronic devices attributable to low production cost, flexibility, processability and ability to pack in small confined space. Polyimide is one of the commercially available polymers used as dielectric in electronic. Polyimide has attracted much attention from electronic industry, owing to their excellent properties such as good insulation, high thermal and chemical stability, good mechanical property and flexibility (Sroog, 1991, De Abajo and De la Campa, 1999). Despite many advantages in dielectric field, polyimide possesses low dielectric constant ($k = 2.8-3.2$) (Ahmad, 2012) which limits its application in high-k application. High k application, which favours high dielectric constant, usually use inorganic or ceramic-based dielectrics because they offer much higher dielectric constant comparing to polymer-based dielectric. However, ceramics usually have low breakdown voltage, high fragility and

brittleness which limit the advancement of ceramic-based dielectric in miniaturization and flexible electronic application (Arbatti et al., 2007; Wang and Wu, 2013).

Hence, polyimide/ceramic composites were developed in order to acquire the exceptional combination properties of both polyimides and ceramics. Introducing ceramic fillers into polyimide matrix allows the polyimide/ceramic composites to have higher dielectric constant than that of conventional polyimide, in the meantime, they are still able to retain their processability and flexibility (Xie et al., 2005). Ceramic fillers such as Al_2O_3 , BaTiO_3 , TiO_2 and ZrO_2 were incorporated into polyimide matrix and found to enhance dielectric constant of the composite when weight percent of fillers increased (Alias et al., 2011; Wang et al., 2009; Zha et al., 2010; Li et al., 2015). For instance, Xie et al. (2005) reported that dielectric constant of the composite with 50% volume fraction of BaTiO_3 was increased by nine times at frequency 10kHz, comparing to that of pure polyimide when BaTiO_3 particles were introduced to polyimide matrix with an aid of 3-amino-propyl-triethoxysilane coupling agent. Similarly, Wang et al. (2009) was also able to tremendously raise dielectric constant value of composite when they prepared polyimide/ BaTiO_3 composite film with a help of a modifier 1-methoxy-2-propyl acetate. Furthermore, the modifier 1-methoxy-2-propyl acetate was used to achieve highly dispersed BaTiO_3 suspension and improve interaction between BaTiO_3 and polyimide. However, large amount of fillers content in the composite was usually needed in order to achieve high dielectric constant, which consequently increase in particle aggregation, void, and impurity presented in the composite. As a result, it caused the growth of unwanted effect such as dielectric loss.

In recent years, one-dimensional (1D) materials such as fibers, nanowires, nanotubes have been extensively used as a filler in the composite due to their small size, high surface-to-volume ratio, high density of surface sites, and unique chemical and physical properties (Wu et al., 2015; Wang et al., 2015c; Tang et al., 2014; Misiego and Pipes, 2013). In comparison to spherical filler particles, filler nanofibers with larger aspect ratios as well as

the longitudinal axis could improve dielectric constant of composite more efficiently at the lower loading content of fillers in the composite (Wu et al., 2015; Wang et al., 2013).

Electrospinning is one of the promising technique used to produce one-dimensional material such as nanofibers because it is a simple and an effective method for ceramics, polymers, and composites (Li and Wang, 2013). Particularly, ceramic nanofibers such as BaTiO₃, TiO₂ and ZrO₂ have been successfully synthesized using electrospinning technique (Wang et al., 2015a; Tekmen et al., 2008; Wang et al., 2015b).

1.2 Problem statements

Polyimide/ceramic composites have attracted attention from many researchers due to their ability to improve dielectric constant as ceramic filler content increased. However, dielectric loss also rose along with addition of filler. In previous research conducted by Rock et al. (2012), polyimide/BaTiO₃ nanocomposites with nanoparticle content of 10% volume fraction (~ 32 wt%) had dielectric constant 6 at 1 MHz, which was about 1.5 time compared to that of pure polyimide. Meanwhile, the dielectric loss of the nanocomposite with same filler content also rose to 0.02 at 1 MHz. Apparently, an increase in the amount of filler was also responsible for the rise of dielectric loss in the composite. Thus, an attempt is made to design and improve the technique of composite preparation that are expected to produce composites with higher dielectric constant and lower dielectric loss. The target is to obtain the composites with filler content less than 32 wt% that could achieve higher or comparable dielectric constant of 1.5 times of pure polyimide with dielectric loss below 0.02 at 1MHz.

Nanofibers were found to efficiently improve the dielectric constant of composite with lower loading content comparing spherical fillers. Moreover, it could minimize the unwanted effect occurred when the amount of nanofibers increased in the composite (Wu et al., 2015; Wang et al., 2013). BaTiO₃, TiO₂ and ZrO₂ are commonly used to enhance dielectric and electrical properties of the polyimide due to their high dielectric constant and

low dielectric loss as well as good thermal stability (Wang et al., 2015c; Liu et al., 2013; Wang et al., 2008).

In this study, the ceramic fillers namely BaTiO₃, TiO₂ and ZrO₂ were produced in nanofiber form via sol-gel process and electrospinning followed by heat treatment before incorporating into polyimide matrix derived from 2,2-Bis[4-(4-aminophenoxy)phenyl]propane (BAPP) and 3,3',4,4'-Biphenyltetracarboxylic dianhydride (BPDA). The synergistic effect of the composite films ensure an improvement of dielectric properties while maintaining the mechanical integrity of the product.

1.3 Objectives of the study

Overall, this study focuses on preparation and characterization of PI/Ceramic nanofibers composite films in which ceramic nanofibers (BaTiO₃, TiO₂ and ZrO₂) were produced by sol-gel process, electrospinning and calcination. The composites were expected to display enhancement of dielectric constant with increasing in weight concentration of fillers while dielectric loss remained relatively low.

The objectives of this study are simplified as follows.

- 1 To synthesize and produce BaTiO₃, TiO₂ and ZrO₂ nanofibers via sol-gel process and electrospinning accompanied by heat treatment.
- 2 To prepare PI/ceramic nanofibers using *in-situ* polymerization and ultrasonic treatment.
- 3 To investigate the chemical, crystal phases, dielectric and thermal properties of PI/ceramic nanofibers composite films with different types of ceramics, uniformity and their weight concentration.

1.4 Scope of the study

This research focused on producing ceramic nanofibers via electrospinning at ambient condition for preparation of polyimide/ceramic nanofibers using *in-situ*

polymerization. Morphology, crystal phases and chemical structure of nanofibers were determined by SEM, XRD and FTIR, respectively. The effect of ceramic nanofibers on dielectric properties (dielectric constant and dielectric loss) of polyimide/ceramic nanofibers composite films were investigated at room temperature at frequency range from 100Hz to 1MHz. In addition, SEM, XRD, FTIR, DSC and TGA were conducted on the composite films in order to study filler dispersion, crystal phases, chemical structures and thermal stability of the composite films at different filler loadings.

CHAPTER TWO

LITERATURE REVIEW

2.1 Dielectric material

Dielectric materials are basically insulators that can be polarized to form electrostatic dipole under an influence of electric field. The insulated materials consist of positive and negative charge balance each other, resulting in electrical neutrality. Their electrical neutrality allows them to prevent electric current passing through the material (Kuffel et al., 2000).

There are four forms of dielectric material which are solid, liquid, vacuum and gas. However, only solid and liquid dielectric have been studied broadly (Von Hippel, 1954). Liquid dielectrics are usually used in various applications such as high voltage application, capacitor and transformer. For instance, petroleum oils are frequently used as liquid dielectric (Naidu and Kamaraju, 2013). Solid dielectric can be divided into two categories which are inorganic and organic. Alumina, Barium titanate and mica are examples of solid inorganic dielectric. Large polymer molecules, which normally have molecular weights more than 600, can be considered as solid organic dielectric. Some common types of organic dielectric materials are polyethylene (PE), polypropylene (PP), epoxy, poly(vinylidene fluoride) (PVDF), polyimide (Whitaker, 2007; Dang et al., 2008; Zhang et al., 2014). In recent year, polymer-inorganic dielectric composites have caught attention of many researchers because their desired properties which convention dielectric materials cannot achieve (Zhang et al., 2014; Li et al., 2015).

Properties of dielectric materials resist the passage of current attributed to their large energy band gap (5 to 7 eV). Only an extremely small conduction or loss current can pass through when a dielectrics influenced by electric field (Bartnikas, 2000). Normally, conductivity of dielectric material will increase if temperature increases under unstable condition where heating rate is greater than cooling rate (Kuffel et al., 2000). Leakage charge

in the dielectrics generally occurs at critical field and mostly happens on high-k dielectrics than do on low-k dielectrics because high-k material has ability to store more charge and become conductive at certain magnitude of applied field. The leakage charge in dielectric materials can lead to dielectric breakdown (Subodh et al., 2007; Naumann, 2008). There are many factors that are able to influence critical applied field of materials such as dielectric geometry, shape and materials of the electrode, ambient condition and time variation of electric field (Ku and Liepins, 1987; Pollock, 1993; Smyth, 1955; Moulson and Herbert, 2003).

2.2 Dielectric polarization

Dielectric polarization occurs when there is a relative swift of positive and negative charges in the material to form dipoles moment under the influence of electric field. The positive and negative charges (q) are separated by certain distance (d) and dipole moment (p) can be expressed as $p = qd$ (Kuffel et al., 2000; Naumann, 2008). The electric dipole moment obtained by an atom or a molecule under the effect of an electric field is proportional to the applied field. This proportionality constant is called the polarizability (α) which is also a measure of an ability of material for responding the electric field. The polarization P is well defined as the electric moment per unit volume of the dielectric and is stated as follow

$$P = N\alpha E \quad (2.1)$$

where, N is the numbers of particles in unit volume (Pollock, 1993; Sirdeshmukh et al., 2006).

Generally, different mechanisms may induce the polarization or electric moment. Callister (2007) proposes that there are four possible types or sources of polarization which are electronic, ionic, orientation and space charge polarization as shown in Figure. 2.1. Therefore, there are also four possible polarizabilities whose summation equals to total polarizability (α) which expressed as

$$\alpha = \alpha_e + \alpha_i + \alpha_d + \alpha_s \quad (2.2)$$

where,

α_e = electronic polarizability

α_i = ionic polarizability

α_d = dipolar polarizability

α_s = space charge polarizability

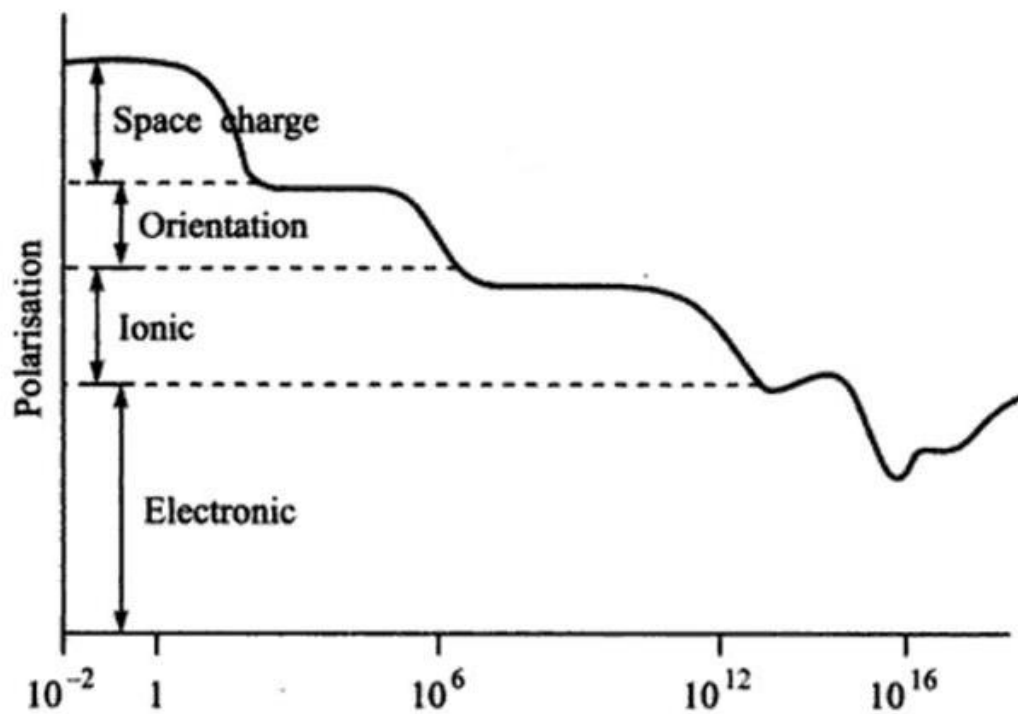


Figure 2.1 Frequency dependence of polarization process (Rajendran, 2010)

The electronic polarizability is one of the main polarizability mechanisms since it occurs in all dielectric materials when they are affected by electric field. It even exists at high frequency range where the other three polarizability are absent. The electronic polarizability is an outcome arisen from shifting the position of the negatively charged electron's orbit from the center relative to positive charged nucleus after affected by electric field (Callister, 2007; Ku and Liepins, 1987; Viswanathan, 2006). The deformation of the

electron's orbit moves its center from the positive charged nucleus, resulting in a dipole moment (Smyth, 1955; Ku and Liepins, 1987).

Ionic polarizability occurs only in materials which possess ionic crystal such as NaCl, KCl, and LiBr (Kasap, 2006; Callister, 2007). In the presence of applied field, net dipole moment is a result of displacement of cations to one direction, and anions to an opposite direction parallel of applied field (Callister, 2007). When there is no applied field, net dipole moment value is basically zero because cations and anions cancel each other (Kasap, 2006; Viswanathan, 2006). Each ion also consists an electron core that is shifted by applied field, relative to its positive nucleus. Hence, electronic polarization also contributes to ions polarization in considerably much small magnitude, comparing to ionic contribution in the solid (Kasap, 2006).

Orientation or dipolar polarizability can be found only in materials consisting permanent dipoles such as polymeric substances and dipolar ceramics. Under normal circumstance, dipoles existing in the polar materials, orient randomly with no net dipole moment and polarization. By applying an external field to the materials, the permanent dipoles tend to change their orientation along the direction of the applied field, resulting in net dipole moment and polarization (Ku and Liepins, 1987).

Space charge polarizability, also known as interfacial polarizability, occurs due to the accumulation of mobile charges derived from contaminants or irregularities within dielectric materials. Trapped electrons and holes, defects such as grain boundaries, voids and dislocation are the cause of the charges accumulating on the surface of dielectric materials, leading to space charge polarization. The occurrence of the space charge polarization is only at very low frequencies as displayed in Figure 2.1 (Sirdeshmukh et al., 2006; Barlow III and Elshabini, 2007).

2.3. Dielectric constant

The dielectric constant (k) of material is a measure of electrostatic energy stored in the material per unit volume for a given voltage. The value of the dielectric constant is a ratio of capacitance of capacitor with a given dielectric material to capacitance of the same capacitor without dielectric in a vacuum as shown in Eq. 2.3.

$$k = \frac{C}{C_o} \quad (2.3)$$

where, C is the capacitance of the dielectric material and C_o is capacitance of vacuum (Smyth, 1955). Thus, value of capacitance of material correlates with dielectric constant of the material. Dielectric constant corresponds to the ability of dielectric material to polarize, and relates to permittivity of material. Permittivity is described as a quantity of electrical energy stored in a substance in an electric field. (Ku and Liepins, 1987). Pollock (1993) states that permittivity determines the ability of material to be polarized when influenced by electric field. The electric field in the material is reduced due to alignment of dipole moment in material. As the result, dielectric material reduces the field upon polarization. Relative permittivity is another technical term of dielectric constant defined as a factor by which the electric field between the charges is decreased relative to vacuum. It is a ratio of the permittivity of a substance to the permittivity of a vacuum as shown in equation (2.4).

$$k = \frac{\epsilon}{\epsilon_o} \quad (2.4)$$

where k is the dielectric constant of material, ϵ is the permittivity of the dielectric material and ϵ_o is the permittivity of vacuum (Smyth, 1955). Table 2.1 show the dielectric constant and dielectric loss of various materials.

Table 2. 1 Dielectric constant and dielectric loss of selected materials at 1 kHz and room temperature

Material	Dielectric constant (k)	Dielectric loss (tan δ)	Reference
Polyimide (Kapton HN)	3.5	0.002	(DuPont Kapton, 2011)
Barium titanate (BaTiO ₃)	>1000	0.086	(Zhang et al., 2013)
Rutile titanium oxide (TiO ₂)	147	0.001	(Kim et al., 2006)
Zirconium oxide (ZrO ₂)	32-42	0.010	(Thompson et al., 1992)

Generally, temperature and frequency affect the dielectric constant of most materials except for some material such as quartz, Styrofoam, and Teflon, whose dielectric constants remain stable (Whitaker, 2007). Dielectric constant is significantly varied when subject to temperature variation due to effect of heat on orientation polarization. As the temperature increases, it will be difficult for molecules aligning since thermal motion increases by heat energy. The value of dielectric constant is higher at low frequency than at high frequency due to low-frequency polarization mechanisms such as interfacial and dipolar polarization. As the result, large capacitance values are easier to achieve at low frequency. At high frequencies, on the other hand, obtaining large capacitances as well as maintaining an acceptable low dielectric loss is more difficult (Kasap, 2006).

2.4 Dielectric loss

Dielectric loss is the energy lost which is dissipated in form of heat during the polarization process in the presence of an alternating field (Naumann, 2008). All of these losses are dependent to temperature and frequency. When the dielectric generates heat faster than it can dissipate, the conductivity and dielectric loss start occurring because of a rise in temperature. For low frequency (below 1MHz), major contribution to heat generation is dielectric loss, while at higher frequencies, electrode resistance plays a significant role

generating heat to dielectric (Moulson and Herbert, 2003). Sirdeshmukh et al. (2006) suggested that conduction loss and relaxation effect are two main causes, contributing to the dielectric loss within a dielectric. In conduction loss, a flow of charge through the material under influence of an applied field, causing dissipation of energy which contributes to dielectric loss. Dielectric loss due to relaxation effect occurs when the polarization lags behind the applied field, resulting in heat due to the interaction between the field and polarization of the dielectric. It is exceptionally high around resonance frequencies of the polarization mechanisms as illustrated in Figure 2.2 (Sirdeshmukh et al., 2006; Barsoum, 2003).

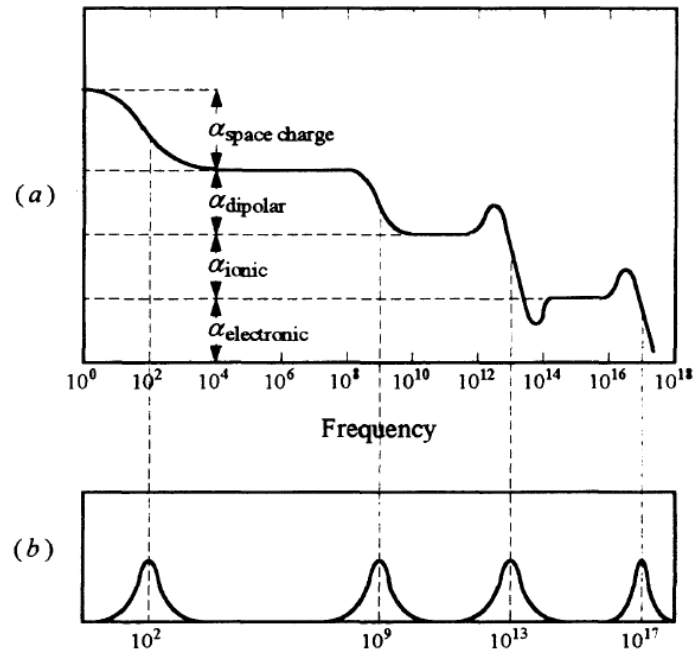


Figure 2.2 Frequency dependence of (a) dielectric constant and (b) dielectric loss (Barsoum, 2003)

Some impurities presence in the dielectric material could increase conductivity. This type of impurities is able to cause a significant increase of dielectric loss (Barsoum, 2003). The lower the dielectric loss the more effective the dielectric materials are since it would ensure low power loss for a good electric material.

2.5 Dielectric application

Most of dielectric applications are used in fabricating capacitor in which high dielectric constant materials are preferable in order to maximize energy storage. Dielectrics are also utilized as transformer, insulator such as wire and cable dielectric amplifier, piezoelectric transducers, resonator and memory devices (Von Hippel, 1954; Subodh et al., 2007). In some applications such packaging materials, printed circuit board materials and ultra-large-scale-integration (ULSI) circuit, require low dielectric constant due to the interconnect capacitance time delay, line-to-line crosstalk noise and power dissipation (Maier, 2001; Grill et al., 2014).

Currently, dielectric polymers or ceramics are used commercially for the conventional dielectric capacitor. An energy density in the conventional capacitor usually is 10^{-2} to 10^{-1} Wh/kg (Yao et al., 2011; Sarjeant et al., 1998). High dielectric constant and high electrical breakdown strength are essential for improving the energy density (Dang et al., 2013). Polymers such as aromatic polythiourea (ArPTU), polyimide (PI), and poly(vinylidene fluoride) (PVDF), are known for their super-high breakdown strength, low fabrication temperature, thermal resistance and good flexibility (Wu et al., 2013; Xu et al., 2016; Li et al., 2010). Although these polymers exhibit many good features for capacitor, there is a drawback for enhancement of energy storage density due to their low dielectric constant. In contrast, some ceramic such as BaTiO₃, TiO₂ and ZrO₂, on the other hand, demonstrate high relative permittivity. Hence, the development of nanocomposite film, based on polymer and high dielectric constant inorganic nanoparticles is needed in order to improve the energy density of capacitor (Dang et al., 2008; Li et al., 2009; Tsai and Liou, 2015).

2.6 Polyimide

Polyimides are a special class of polymer containing an imide group. The structure of polyimide can be linear aliphatic polyimide and aromatic polyimide (Gary and Zoubeida, 2006). Among them, aromatic polyimide is the most used polyimide due to its great

thermostability, outstanding mechanical properties, superior chemical resistance and high glass-transition temperature ($T_g = 250\text{ }^{\circ}\text{C}$) (De Abajo and De la Campa, 1999; Liaw et al., 2012; Sroog, 1991). The linear and stiff cyclic backbone of aromatic polyimide permit a good molecular ordering which contributes to thermal stability and good solvent resistance (Dunson, 2000). The highly symmetrical and polar groups make the fully aromatic polyimides to have rigid chains and strong inter-chain interaction. As the result, the polyimides have low solubility and no melting point (Liaw et al., 2012).

Polyimides have been extensively used in many applications such as spacecraft application, flexible electronics and biomedical application (Watanabe et al., 2012; Cheung et al., 2007; Tsai and Liou, 2015). Polyimides possess the attractive combination of rigid and fairly insoluble properties which are suitable for interconnect and electronics packaging application (Gary and Zoubeida, 2006). Other favourable applications of polyimide are in dielectrics for integrated-circuit design owing to their good thermal stability, high mechanical strength and excellent radiation properties. These combination of properties are able to solve some concerned issues in dielectrics such as the resistance-capacitance (RC) time delay, cross talks and power dissipation (Deligöz et al., 2005; Lin and Wang, 2007; Chang et al., 2006).

2.6.1 One-step method synthesis

One-step method synthesis is usually used on the polyimides, which are able to dissolve in organic solvents. In this process, high-boiling organic solvents such as nitrobenzene and α -chlornaphthalene are used for dissolving both dianhydride and diamine. Then, the solution is stirred at elevated temperature around 180°C to 220°C . The chain development and imidization basically occur in spontaneous manner under these condition. During the imidization, the water is generated and permitted to distil from the reaction mixture

An advantage of one-step method is that it can be used in polymerization of unreactive monomers such as phenylated dianhydrides. These types of monomers are not able to yield high molecular weight poly(amic acid). However, they react rapidly at elevated temperatures and achieve high molecular weight polyimide. Another fascinating benefit of the one-step method is that higher degree of crystallinity of polyimide can be obtained, comparing to the two-step method. (Harris, 1990).

2.6.2 Two-steps method synthesis

Two-step synthesis remains the most widely practice method for decades, and was discovered and developed by Dupont in 1950s (Sroog et al., 1965). In the first step, PAA solution is formed by allowing an aromatic dianhydride with an aromatic diamine to react in a dipolar aprotic solvent, generally N-methylpyrrolidone (NMP). The second step involves curing the PAA solution by heating up to 400 °C to release water or alcohol molecule from the amide ester groups. As a result, the thermally stable cyclic imide rings are formed through imidization process. (Strong, 2008; Licari, 2003). The reaction scheme of two-steps method is demonstrated in Figure 2.3.

Synthesis process of polyimide is influenced by many factors which therefore also affect the final properties of polyimide. Higher concentration of monomers is likely to yield higher molecular weight of PAA because a lower amount of solvent can reduce the side effects caused by impurities in solvent, interfering with the growth of molecular weight (Dine - Hart and Wright, 1967). PAA was reported to achieve higher molecular weight when the process was done at lower temperature due to the exothermic nature of PAA formation (Sroog et al., 1965; Dunson, 2000). Another important factor affecting the final molecular weight of polyimide is the order of monomers addition. If the dianhydrides are added first into the solvent, small amount of moisture presented in monomers and solvent will react with anhydride endgroups, resulting in dicarboxylic acid. This disturbs the stoichiometric balance between dianhydride and diamine, leading to lower the molecular weight. Therefore, it is

necessary to add solid dianhydrides into the solution with completely dissolved diamines in dipolar aprotic solvent because the dianhydrides can react faster with diamines than moisture content in solvent (Harris, 1990).

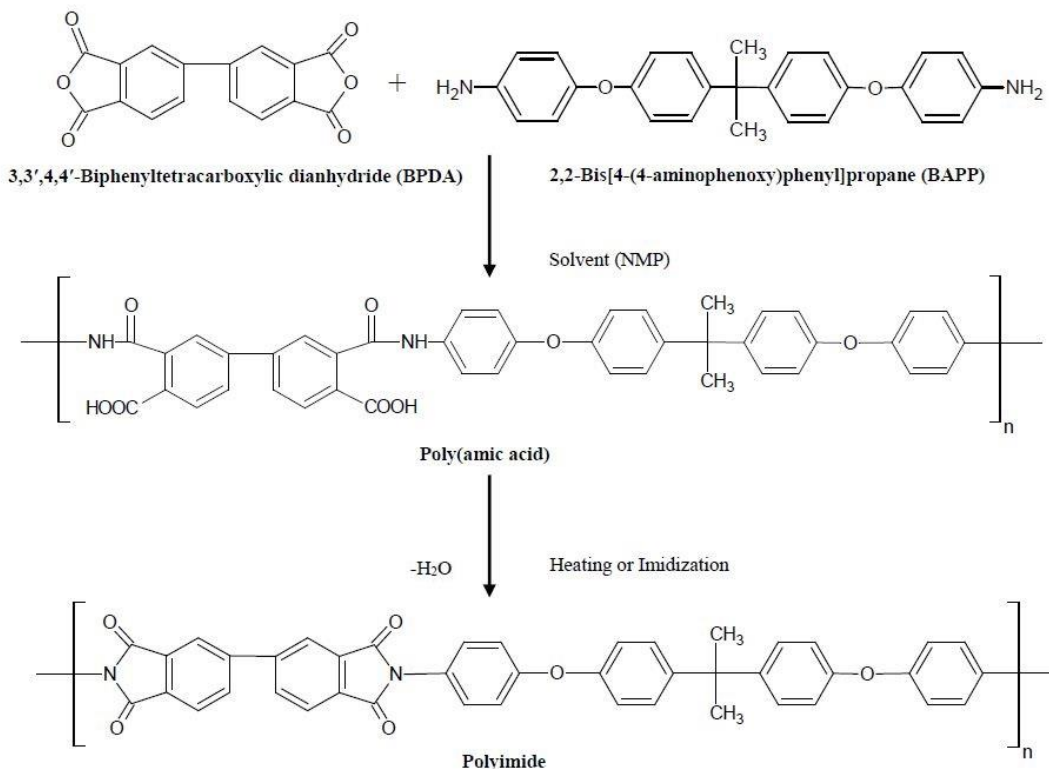


Figure 2.3 Reaction scheme of poly(amic acid) and polyimide

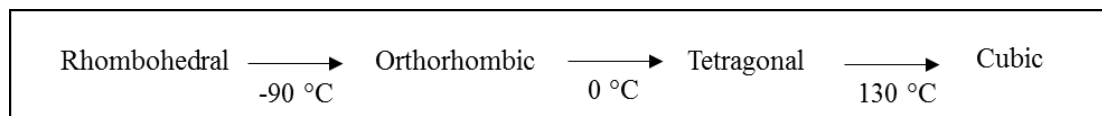
Formation of intermediate PAA is initiated when dianhydrides are added into solution containing diamines and dipolar aprotic solvent. This formation occurs because the amino group from diamines conducts the nucleophilic attack on the carbonyl carbons of the anhydride group (Dunson, 2000). The PAA solution is usually cured or imidized by heating in solid state to 250–400°C in second step in two-step method of polyimide synthesis. In addition, PAA is often casted on clean and dry disk or spin-coated to obtain thin film before curing (Harris, 1990; Kim et al., 2009). There are many types of thermal cycles to ensure the imidization of PAA closed to 100%. A type of thermal cycles consists of gradually heating to 250–350°C, depending on glass transition and stability of polyimide (Harris, 1990; Takekoshi, 1996). Another type of heating cycles is the most commonly used. It involves

drying the sample in the oven at temperature range 50°C–100°C for certain period of time in order to evaporate solvent. Then, the sample is heated in furnace at 100°C, 200°C and 300°C for an hour each temperature (Liu et al., 2008a; Dang et al., 2008; Harris, 1990).

2.7 Ceramic fillers

2.7.1 Barium titanate

Barium titanate (BaTiO_3) is titania-based ceramic with perovskite crystal structure. BaTiO_3 has rhombohedral, orthorhombic, tetragonal and cubic phases. The phase transition from rhombohedral to cubic phase occurs upon heating as following (Barsoum, 2003).



In cubic phase as shown in Figure 2.4, Barium atoms are located at all eight corners of a cubic-shaped unit cell, while titanium atom stays at the center of the cell, surrounded by 6 Oxygens octahedron (Barsoum, 2003; Callister, 2007). In tetragonal phase, BaTiO_3 has a distortion of cubic perovskite structure in which the unit cell elongates in c-axis and Ti^{+4} moves from its centrosymmetric position along the same axis as elongation of unit cell as shown in Figure 2.4. This behaviour creates a permanent electric dipole and makes tetragonal BaTiO_3 classified as ferroelectric material (Jaffe et al., 1971; Strukov and Levanyuk, 1998). The ferroelectric characteristic and high dielectric constant (2000-5000 at room temperature) allow BaTiO_3 become a dominant dielectric material in various applications in electronic industry (Wang, 2002; Viswanathan, 2006; Vijatović et al., 2008).

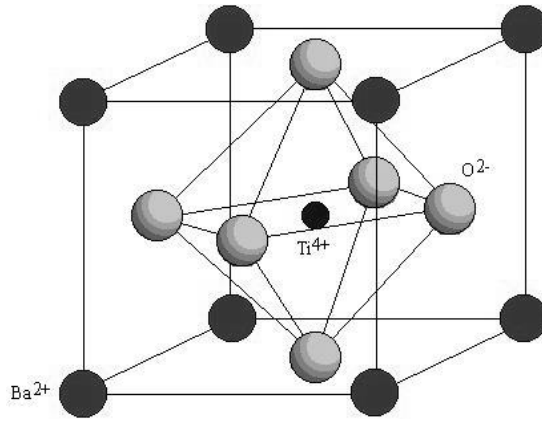


Figure 2.4 A unit cells for the perovskite structure of BaTiO₃ (Viswanathan, 2006)

BaTiO₃ has many applications in electronic industry such as flexible piezoelectric devices, a PTC (positive thermal coefficient) materials, a pyroelectric sensor, capacitor and microwave dielectric ceramic, a variety of electro-optic devices and energy storage devices (Wang, 2002; Wang et al., 2015a; Gong et al., 2014). Furthermore, BaTiO₃ also has a wide range of application in semiconductors, positive ultrasonic transducers. Thus, BaTiO₃ has become one of the most important ferroelectric ceramics (Vijatović et al., 2008).

2.7.2 Titanium oxide

Titanium Oxide (TiO₂) exists in three different crystal structures which are rutile (tetragonal), anatase (tetragonal) and brookite (orthorhombic) as seen in Figure 2.5. Rutile is the most thermally stable form. Anatase and brookite phases are less stable than rutile phase and could transform to rutile phase with applied heat (Khataee and Mansoori, 2011). Rutile has a body-centred tetragonal unit cell, in which Ti⁴⁺ is surrounded by an octahedron of 6 oxygen atoms. In anatase, the three dimensional framework is formed by edge-shared bonding among TiO₆ octahedrons arranged in zigzag chains. In brookite, the TiO₆ octahedra are arranged in the three dimensional framework by sharing both edges and corners and constructing an orthorhombic structure (Khataee and Mansoori, 2011). Notably, Rutile-structured TiO₂ possesses exceptionally high dielectric constant (over 100 at room temperature) among the three crystal structures (Kim et al., 2006; Marinell et al., 2013).

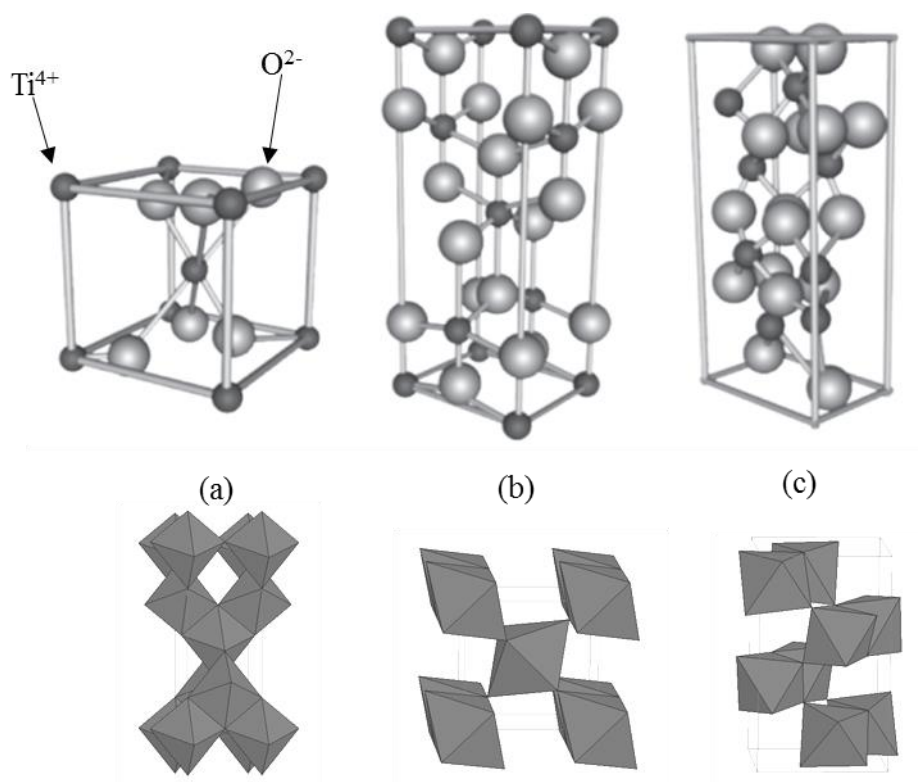


Figure 2.5 Unit cells (top) and crystal structures (bottom) of (a) rutile, (b) anatase and (c) brookite (Khataee and Mansoori, 2011)

Titania has been one of the most widely used materials in numerous applications including pigment, sensor devices, dye sensitized solar cells, photocatalysts and supercapacitors (Varghese et al., 2003; Pastore et al., 2016; Liang et al., 2017; Prasannalakshmi et al., 2016). Furthermore, TiO_2 also has been utilized in biomedical application owing to its brilliant biocompatibility, high chemical stability, nontoxicity and low cost (Junkar et al., 2016). As rutile TiO_2 exhibits high dielectric constant, it is widely used in capacitor fabrication and microelectronic devices (Khataee and Mansoori, 2011).

2.7.3 Zirconium oxide

Zirconium oxide or zirconia is the most stable oxide of zirconium and also one of the most important ceramic materials. ZrO_2 can be found in three crystal phases which are monoclinic, tetragonal and cubic as shown in Figure 2.6. Monoclinic phase is stable at low temperature and go through a reversible transition to the tetragonal phase at 1170°C . The

tetragonal phase can be stable up to 2370°C and above this temperature, the phase transition from tetragonal to cubic phase occurs. The cubic phase become stable until it reaches melting point of zirconia at 2680°C (Barsoum, 2003). The transition of the phases is shown as follows.

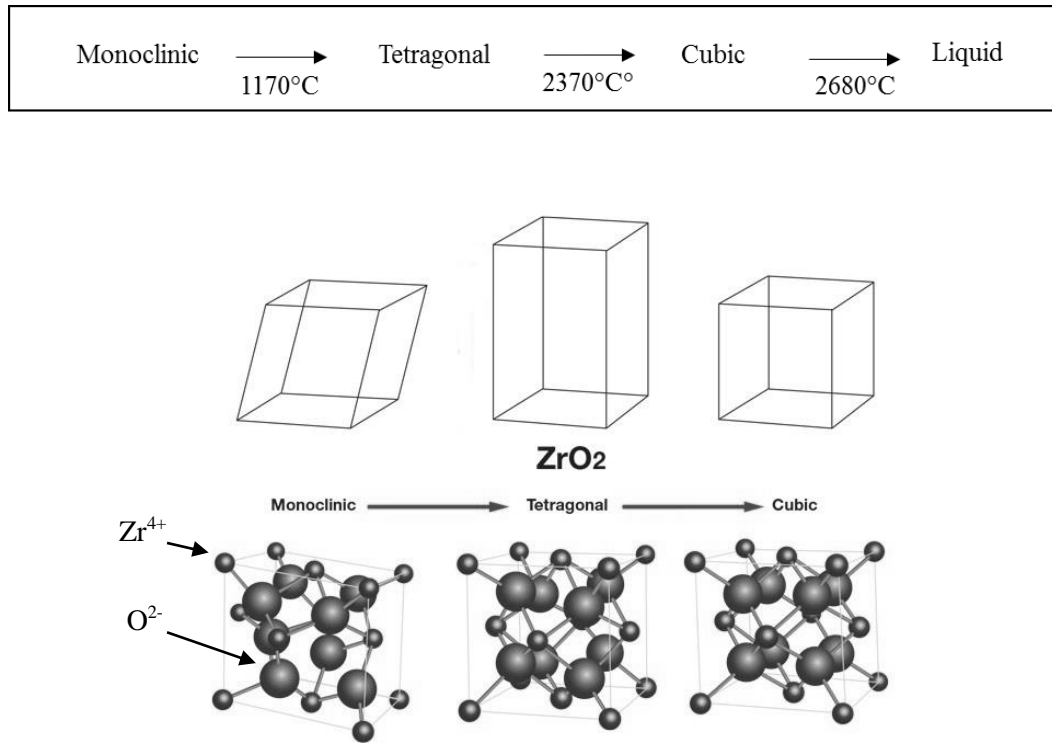


Figure 2.6 Crystal phase and unit cell of Zirconium oxide (Glidewell Laboratories, 2016)

Zirconia is a remarkable ceramic materials which possess superior thermal stability with high melting point. These features make zirconia become one of the best refractory materials. In addition, ZrO₂ also have chemical inertness property which make zirconia useful in some applications such as heat exchangers, crucibles and pouring nozzle (Garvie, 1970). Significantly, Zirconia is oxygen-ion conducting material which widely used in various application including oxygen sensors, oxygen pumps, fuel cell (Brailsford et al., 1997; Ramamoorthy et al., 2003; Singhal, 2002). Tetragonal Zirconia has a considerably high dielectric constant ($k \sim 47$), which enable its application in high-k dielectric materials including Metal-Insulator-Metal (MIM) Capacitor, Metal oxide semiconductor (MOS)

device and field-effect transistor (FET) (Ferrand et al., 2013; Wu et al., 2011; Wang et al., 2016).

2.8 Polyimide/ ceramic composites

Polymer/ceramic composite are organic/inorganic composite consisting of polymer matrix and ceramic fillers. Extensive study has been conducted on this hybrid composites over past decades due to their superior combination properties which cannot be found in conventional polymer and ceramic (Chung, 2010). Among various types of polymer used for polymer/ceramic composites, polyimide has stood out and attracted attention from both academic research and industry attributed to its unique characteristics, incredible heat and chemical resistance, good mechanical performance as well as other outstanding properties as described in Section 2.6. Throughout the years, there are various attempts to improve dielectric constant of polyimide by introducing ceramic fillers with different shape and size to polyimide matrix. BaTiO₃, TiO₂ and ZrO₂ are among the common ceramic fillers used in polyimide/ceramics composite. BaTiO₃ possesses very high dielectric constant owing to its perovskite structure. Hence, it is usually chosen as a filler for enhance dielectric constant of polyimide. For instance, Wang et al. (2015c) have incorporated BaTiO₃ nanowires into polyimide to increase dielectric constant, which in turn enhance energy density storage of the composite film. On the other hand, TiO₂ also has many good properties as mentioned in Section 2.7.2. Thus, Liu et al. (2013) have introduced TiO₂ nanoparticles into polyimide matrix in order to improve electrical and mechanical properties of the composites. Lastly, ZrO₂ was used as a filler in the polyimide composite by Wang et al. (2008) for electronic application due to its high wear resistance, chemical endurance and heat resistance.

2.8.1 PI/BaTiO₃

PI/BaTiO₃ composites are one of the most promising polyimide/ceramics composites which focus on dielectric constant enhancement due to the enormous dielectric constant of BaTiO₃ (Chen et al., 2013). Liu et al. (2008) conducted the study on PI/BaTiO₃ by mixing

PAA with BaTiO₃ modified by coupling agent (3-aminopropyltriethoxysilane, APTS) before heat treatment for PI/BaTiO₃ composite. They found that the dielectric constant of composite improves with the increase in filler content. Another research carried out by Dang et al. (2008) investigated on the method of incorporation between Polyimide and BaTiO₃. They claimed that *in-situ* polymerization prepared by mixing diamine and BaTiO₃ in solvent first before slowly adding dianhydride into the solution, were more efficient for enhancing dielectric constant comparing to direct mixing between PAA and BaTiO₃. They explained that by slowly adding dianhydride into PAA/ BaTiO₃, PAA oligomers with low molecular weight were able to form and easier to be absorbed onto the surface of BaTiO₃ particles easily at low viscosity than high molecular weight PAA. In recent year, researchers have changed their attention to the one dimensional BaTiO₃ such as nanowire and nanofibers. BaTiO₃ nanowires and nanofibers were used in PI/ BaTiO₃ composite and proven not only to improve dielectric constant more efficiently, but also maintain the low dielectric loss of the composite (Wang et al., 2015c; Xu et al., 2016).

2.8.2 PI/TiO₂

PI/TiO₂ composites have been received considerable amount of attention in many applications including electronic devices, high-refractive index materials, highly transparency materials, antireflective application and optical materials (Yu et al., 2011; Huang et al., 2016; Ando, 2009). Feng et al. (2013) studied polarization process of PI/TiO₂ composites and discovered that dielectric constant of PI/TiO₂ composite began to increase when loading of TiO₂ was equal or higher than 5w%. They indicated that TiO₂ particles pinned down the chain motion of PI, leading to the decrease in dielectric constant at lower filler content. Another study conducted by Zha et al. (2010) observed that the dielectric constant and the dielectric loss of the PI/TiO₂ nanocomposite films rose with increment of weight concentration of TiO₂ nanoparticles.

2.8.3 PI/ZrO₂

PI/ZrO₂ composites are also among the interesting hybrid composites which have been noticeably studied and used in applications such as in fabricating flexible capacitor, highly transparent materials and dielectric materials (Wang et al., 2008; Tsai and Liou, 2015). Wang et al. (2008) investigated on the influence of ZrO₂ with the modifier (1-methoxy-2-propyl acetate) on the PI/ZrO₂ composites. Based on their report, ZrO₂ with the modifier helped stabilized ZrO₂ suspension in PAA solution and enhancing interaction between fillers and polyimide. As a result, dielectric constant of PI/ZrO₂ composites with modifier increased with addition of ZrO₂. However, modifier did not help preventing dielectric loss at 1MHz from rising up with increasing in fillers concentration.

2.9 Electrospinning

Electrospinning is an incredible technique used for the formation of one-dimensional nanofibers ranging from few nanometers to several micrometers by using electrical forces. The electrospinning has been known for over a century, but only gained much attention in the last few decades (Cooley, 1902; Bhardwaj and Kundu, 2010). This technique offers a unique capability to produce fibers with high specific surface area, high porosity, large surface-to-volume ratio and small pore size. Furthermore, electrospinning is not only limited to produce nanofibers from a wide variety of polymers, but also has ability to fabricate nanofibers from abundant ceramics and composites (Haghi, 2011; Ramakrishna et al., 2006; Wu et al., 2015). Due to these many advantages, electrospinning have been extensively studied and investigated for exploring their potential applications, such as filtration, optical and chemical sensors, electrode materials, nanocatalysis, energy storage devices, biomedical, optical electronics and biotechnology (Liang et al., 2007; Bhardwaj and Kundu, 2010; Shi et al., 2015).

2.9.1 Set up and operation principle

The main components of electrospinning consist of syringe loaded with suitable polymer solution and equipped with a needle, a syringe pump, a high voltage supplier and

collector plate (usually plate, rotating mandrel and metal screen). The main components usually are set up in either horizontal or vertical direction. Additionally, the electrospinning are commonly conducted at atmospheric pressure with room temperature (Liang et al., 2007; Bhardwaj and Kundu, 2010). Generally, the syringe filled with polymer solution is loaded on the syringe pump, and the needle of syringe is connected to the positive terminal of high voltage supply. The collector plate is connected with the ground in order to create electric field from the needle to collector as shown in Figure 2.7.

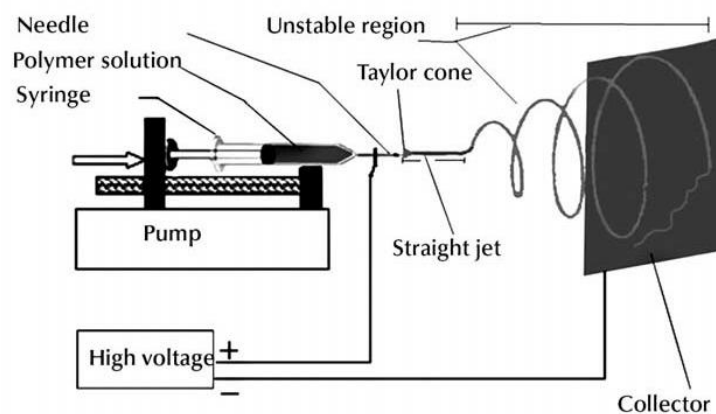


Figure 2.7 Typical electrospinning set up (Haghi, 2011)

In electrospinning process, when the polymer solution is ejected from the syringe through the needle, the droplet of polymer solution at end of the needle is held by its own surface tension before falling down when no electric field. However, when the electric field is applied to the needle, an electrostatic charge acquired from the needle is induced on the liquid surface. Eventually, the repulsive electrostatic forces on the droplet exceed the surface tension forces as the applied electric field increases and reaches critical value or threshold voltage. As a result, an induced charge jet of the solution is ejected from the needle tip to the collector, resulting in formation of a Taylor cone at the tip of needle (Taylor, 1969; Shin et al., 2001). The polymer solution jet travels through the space between the needle and collector with an unstable and rapid whipping motion, causing fibers to elongate and decrease in diameter. Furthermore, the solvent also evaporates due to travelling through atmosphere and the whipping motion or bending instability of the jet, consequently leaving